Design Considerations for High-Voltage High-Current Bi-Directional DC Solid-State Circuit Breaker (SSCB) for Aerospace Applications

Asad Fayyaz*, Zhenyu Wang, Matias Urrutia Ortiz, Tao Yang, Patrick Wheeler
University of Nottingham
Power Electronics, Machines and Control (PEMC) Group, PEMC Building
15 Triumph Road, Jubilee Campus, Nottingham NG7 2GT, United Kingdom
Tel: +44 / (0115) 748 4493
Email: asad.fayyaz@nottingham.ac.uk; zhenyu.wang@nottingham.ac.uk; matias.urrutiaortiz@nottingham.ac.uk; tao.yang@nottingham.ac.uk; pat.wheeler@nottingham.ac.uk
URL: https://www.nottingham.ac.uk/research/groups/pemc/home.aspx

Acknowledgements

This project has received funding from the Clean Sky 2 Joint Undertaking under the European Union's Horizon 2020 research and innovation programme under grant agreement 831877

Keywords

Solid-State Circuit Breaker (SSCB), DC circuit breaker, Solid-State, Fast fault detection, Aerospace.

Abstract

Design of a high-voltage and high-current solid-state circuit breaker (SSCB) for aerospace applications is highly challenging, as the overall system should comply with the most stringent operating environment. In addition, the implemented power semiconductor devices within the SSCB would require excellent thermal performance and efficiency with minimised conduction losses as they always operate during on-state and only break current when there is a fault. The newer generation of the more electric aircraft architecture has a proposed DC link voltage of 2.4 kV (+/- 1.2 kV) which is much higher than the presently used DC link voltage of 540 V (+/- 270 V). The proposed DC SSCB would be rated at 2.4 kV with a nominal current rating of 100 A and would be used for protection and controllability to protect the aircraft's DC grid transmission network. A brief overview of the different elements of a DC SSCB have been discussed here followed by a discussion about the different viable bi-directional SSCB topology configurations. The thermal simulations were carried out in PLECs, which provide the conduction losses and junction temperature dynamics for different switch (Si devices and SiC MOSFETs) types and topologies. Moreover, different figures of merit such as conduction losses, semiconductor weight, and power density are also discussed.

Introduction

In recent years, increased research efforts have been made to take a step forward towards the realisation of the concept of a more electric aircraft (MEA) / All Electric Aircraft (AEA). This is due to growing pressures on the aerospace industry to cut down on their carbon emissions as well as having more efficient lightweight aircraft systems. Such developments within the aerospace industry have been possible due to new emerging enabling technologies which have resulted in viable alternative solutions to replace the existing aircraft power and propulsion systems with more electric solutions. Even though examples of aircrafts such as the Airbus A380 and Boeing 787 which exhibit electrical systems currently exist, there is still a lot that could be done to realise the shift from research-level to commercial level for MEA/AEA on a wider scale [1]. This research forms part of the Ground Demonstrator in which, out of the four turbofan engines within an aircraft, one of them is being replaced with a 2 MW electric motor which would be driven by an on-board 2 MW Generator connected to a Gas Turbine. As per the new proposed aircraft architecture, the AC output of the 2 MW generator would have to be rectified to generate a DC voltage which would have to be connected to a ± 1.2 kV (2.4 kV) DC bus. This DC bus will create a transmission distribution system in order to connect the generator power electronics (AC/DC converter) to the power DC distribution grid. The SSCB prototype, capable of breaking/interrupting DC current, required as part of this work is needed to be rated at DC link voltage of ± 1.2 kV (2.4 kV) with a nominal steady-state operational current rating of 100 A and transient current rating which is 2x the nominal current of 200 A. The SSCB is going to be placed at the output of the AC/DC converter (rectifier) and the start of the DC grid transmission network (i.e. cables) forming the ± 1.2 kV (2.4 kV) DC bus line. The position of the SSCB is highlighted by the red arrow as presented in Figure 1.

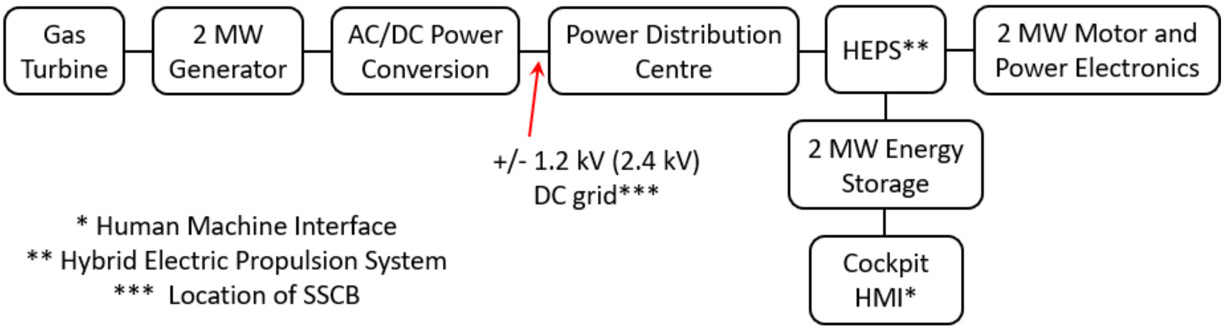

Figure 1: Proposed Serial Hybrid Architecture for the Aircraft

Overview of a Solid-State Circuit Breaker (SSCB) and Bi-Directional Topologies

There are two main elements associated with the design of a SSCB. The first fundamental element is associated with the selection of power semiconductor devices. For SSCBs, the power devices are always going to be in the on-state conduction mode. Therefore, appropriate selection of power semiconductor devices and an investigation of on-state conduction power losses for these devices is critical. Moreover, the devices would also experience current levels considerably higher than the nominal current depending on the overcurrent protection requirements. In this work, 2x the nominal on-state current is being considered; however, the transient current levels could reach as high as 9x the nominal current level as dictated by the DO-160 standard. Secondly, during a transient event in case of device turn-off as a result of over-current detection within the circuit, the back EMF produced by the grid inductance may force the devices to go into avalanche breakdown operation (therefore exceeding the rated blocking voltage of the device). In order to avoid avalanche breakdown operation, devices also require additional separate voltage clamping in order for the energy stored in the grid inductance to be dissipated in the overvoltage protection element and not the power semiconductor device itself.

The second fundamental element of SSCB is the selection of the overvoltage protection element. The relevant features of different power semiconductor devices for designing a bidirectional SSCB are highlighted in Table I below. The forward and reverse conduction of the devices along with their associated forward and reverse blocking capability are to be considered when devising a four-quadrant switch for bi-directional current conduction and voltage blocking capability.

There are three different types of circuit elements that can be used for over-voltage protection: a metal oxide varistor (MOV), transient voltage suppression (TVS) diode, and a snubber. A MOV is a non-linear variable resistor whose resistance is dependent on the applied voltage across it. However, MOVs are susceptible to degradation of its electrical parameter when subjected to repetitive current transients as a result of changes in its microstructure. Most commonly commercially available MOVs are manufactured using Zinc Oxide (ZnO) and are usually known as ZnO Varistors. The typical voltage-current behaviour of a MOV is presented in Figure 2 (a). Another issue of MOVs is that the clamping voltage significantly varies with the current being switched at device turn-off. Some studies into the degradation of MOVs can be found in [2, 3]. Therefore, MOVs are ideal to absorb energy during non-repetitive transient events. If it is predicted to have repetitive over-current transient events during the lifetime of a SSCB, therefore, TVS diodes are more reliable as they possess stable electrical parameters even when subjected to repetitive avalanche breakdown operation. Conversely, a TVS diode is essentially a P-N diode that makes use of the avalanche breakdown feature of the diode. Thus, it is sometimes also known as an avalanche breakdown diode (ABD). The I-V device characteristics for a typical bi-directional TVS diode are presented in Figure 2 (b). Unlike MOV, the avalanche breakdown voltage of a TVS diode does not change significantly with the amount of current flowing through it. However, the TVS diodes have a high cost as compared to a MOV. Both the MOVs and TVS diodes can handle high energy absorption but as also mentioned earlier, the selection criteria would depend on the frequency of over-current transient events expected during the lifetime of a SSCB along with subsequent lifetime reliability considerations. Finally, a snubber circuit within power electronics consists of a resistor connected in series with a capacitor usually termed as a RC snubber. However other types of snubber circuits also exist. Having a snubber circuit would help slow down the dV/dt of the semiconductor device to obtain soft-switching and reduce the switching loss during over-current device turn-off. MOV or TVS Diode can also be implemented together with the snubber circuit. The representation of dV/dt at turn-off with and without snubber is included in Figure 2 (c).

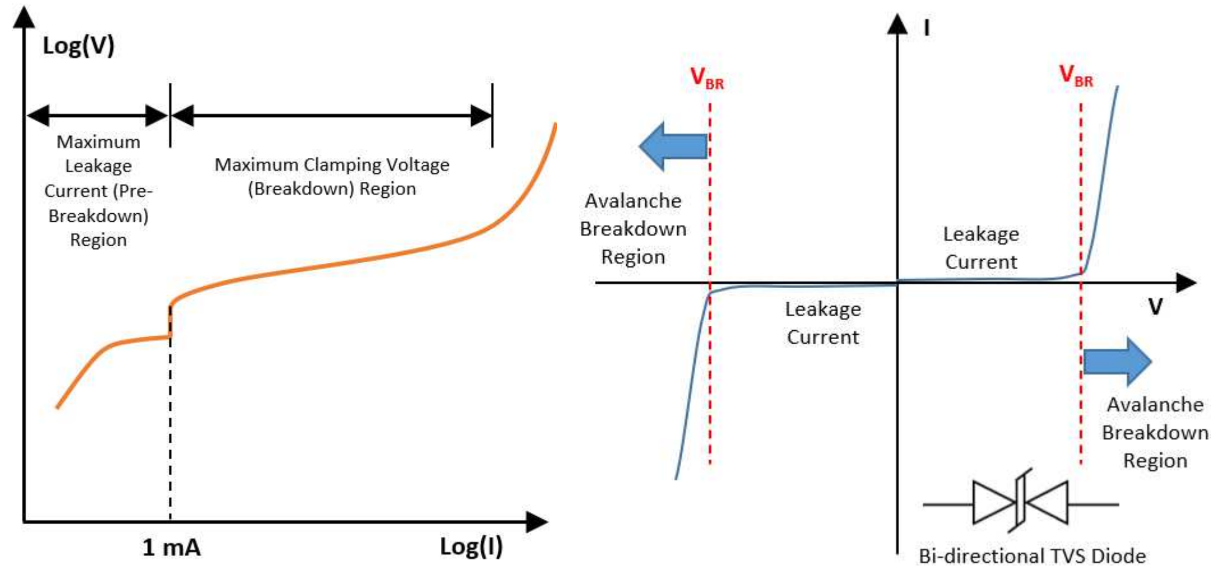

(a): Voltage/Current characteristics of a MOV (b): Current/Voltage characteristics of a TVS Diode

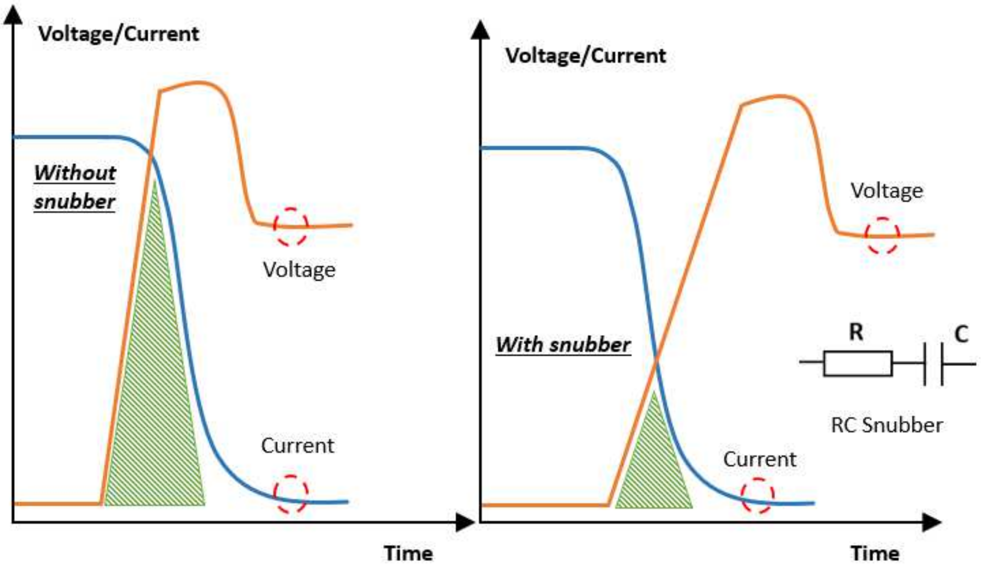

(c) Turn-off switching transient with and without snubber circuit

Figure 2: Characteristic waveforms of different over-voltage protection / TVS elements

Table I: Summary of different power semiconductor devices

	Forward Conduction	Reverse Conduction	Forward Blocking	Reverse Blocking
PiN Diode	Yes	No	No	Yes
Schottky Diode	Yes	No	No	Yes
Thyristor	Yes	No	Yes	Yes
Gate Turn-off Thyristor (GTO)	Yes	No	Yes	Yes (with Symmetrical GTO)
Integrated Gate Commutated Thyristor (IGCT)	Yes	No (Possible with RC-IGCTs)	Yes	Yes (with Symmetrical IGCT)
JFET	Yes	Yes	Yes	No
MOSFET	Yes	Yes (Channel and body-diode)	Yes	No (Possible with anti-parallel diode)
IGBT	Yes	No (But RC-IGBTs are available)	Yes	No
BJT	Yes	No	Yes	No

The typical circuit schematic for a SSCB implemented in a DC distribution system is presented in Figure 3. In Figure 3, the DC source represents the output of the AC/DC power conversion. The SSCB block includes the power semiconductor devices along with the over-voltage protection elements. The R_{DC} and L_{DC} represent the resistance and inductance of the cables respectively used within the DC distribution network. The DC load consists of a resistor (R_{LOAD}) and a capacitor (C_{LOAD}).

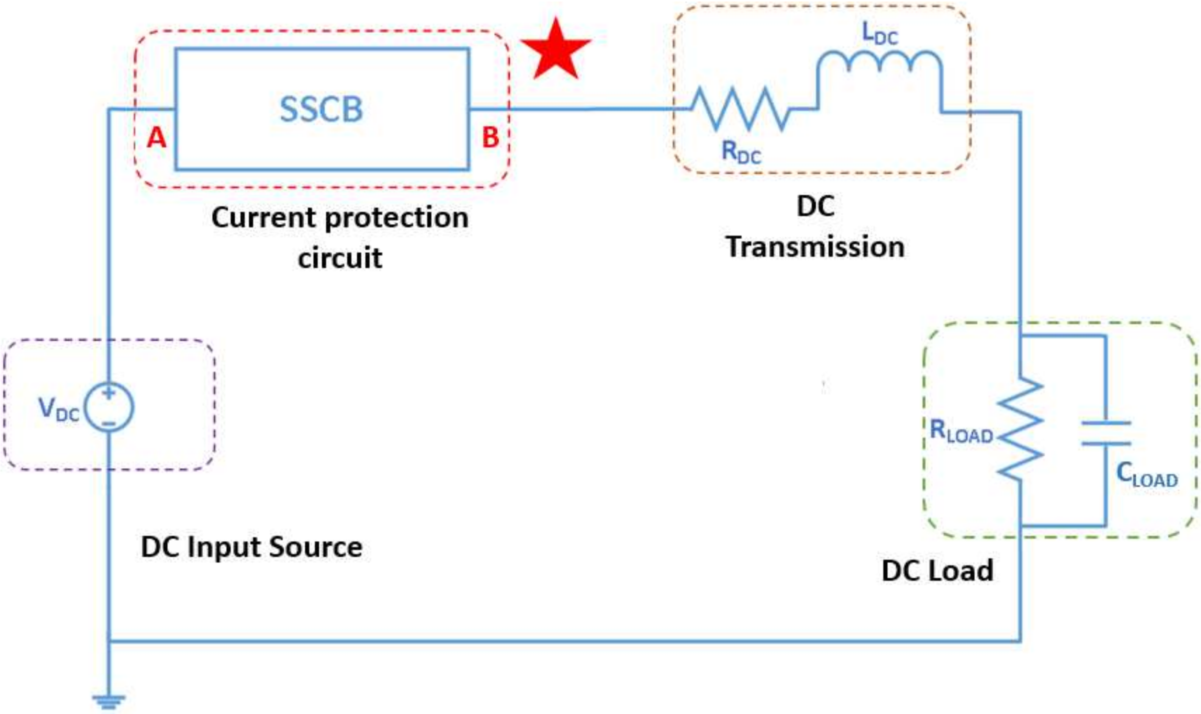

Figure 3: Typical circuit schematic for a SSCB for a DC distribution network

Appropriate selection of the semiconductor devices and their associated heatsink size would also need to take into account the I^2t over-current protection requirements for the SSCB. Most commonly used guidelines for aerospace applications as per the DO-160 document propose overcurrent operation of up to 9x the nominal current [4]. However, other over-current conditions involving operation up to 2x and 4x the nominal current are also considered. Here, in this work, an overcurrent operation of up to 2x the nominal current for 50 ms is being considered.

The bi-directional SSCB could be developed using the semiconductor power devices mentioned in Table I. However, the different topologies for SSCB that are possible would depend on the configuration of the modules which are available for the voltage and current ratings as per the required application specifications. Here, seven different topologies have been selected that could be investigated for this work but other topologies are indeed possible according to the ratings of the power modules that are being selected. Some of the viable topologies are discussed here and their schematics are included in Figure 4. Moreover, all the topologies presented below show MOV as the TVS diode. However, it could also be replaced with a TVS diode as also discussed earlier.

Topology TP1 consists of two gate turn-off thyristors (GTOs) and two diodes. GTOs also require an auxiliary circuit, a resistor and capacitor (connected in parallel) for protection against turn-off voltage [5]. Thyristor-based semiconductor devices such as GTOs used in this topology have superior voltage and current ratings as compared to MOSFETs and IGBTs; therefore, they are of particular interest for very high power SSCBs [6]. However, gate drive circuit design is complex due to the gate drive current and speed requirements for turning off the GTO, which is quite difficult to meet [7]. The series-connected diode is needed as most of the GTOs available nowadays are asymmetric (capable of forward blocking only) as the on-state losses of existing symmetric GTOs (also capable of reverse blocking) are high. During the current conduction (on-state), the upper branch carries the positive current and the lower branch carries the negative current. During the voltage blocking (off-state), the GTO in the upper branch is in forward blocking mode and the diode in the lower arm is in the reverse blocking mode and vice versa.

Topology TP2 consists of two Integrated gate-commutated thyristors (IGCTs) and two diodes. IGCT is quite similar to a GTO but comes with an integrated gate drive circuit. IGCT is usually termed as the “gate-controlled turn-off” switch, which conducts like a Thyristor with really extremely low conduction losses but turns off like a transistor. This makes IGCTs a good choice for high voltage and high current SSCB. However, the complete IGCT modules tend to be quite bulky but indeed the user benefits from the integrated gate-drive circuit. In general, IGCTs also require a snubber circuit when connecting them in series to ensure symmetric voltage distribution between the semiconductor devices. However, for a single IGCT, it is not needed, and instead, the MOV is connected directly in parallel [5]. Here, again, the series-connected diode is needed unless using an asymmetric IGCT. During the current conduction (on-state), the upper branch carries the positive current and the lower branch carries the negative current. During voltage blocking (off-state), the IGCT in the upper branch is in forward blocking mode and the diode in the lower arm is in the reverse blocking mode and vice versa. The diodes would need to have the same reverse voltage blocking capability as the forward voltage blocking capability of the IGCTs. The same also applies to the previous topology TP1.

Topology TP3 has one GTO and four diodes connected in a full diode rectifier configuration. In this topology, either during the positive or the negative current direction, the current flows through two diodes as opposed to just one diode in TP1 and TP2. The full diode rectifier is used to reduce the number of active devices by half to reduce overall semiconductor costs. However, in the long run, the operational costs tend to be high for this type of topology due to the increased costs related to higher power losses during operation [5]. Current flowing through two diodes connected in series means that this topology suffers from higher overall on-state losses due to the losses in the additional conducting diode. During the voltage blocking phase, the GTO is in forward blocking and two out of four diodes would be in reverse blocking mode as dictated by the voltage applied to the SSCB (between point A and B).

Topology TP4 is similar to topology TP3 but it consists of IGCTs as the active device and therefore has similar operation to TP3.

Topology TP5 consists of two IGBTs and two diodes connected using a common emitter configuration [9]. This topology could potentially be implemented using a single module having a common emitter configuration as they are widely available (depending on the voltage and current ratings of the SSCB). It also makes use of a snubber circuit for each active device and a combined MOV in parallel for both IGBTs for over-voltage protection at turn-off. During the current conduction (on-state), the positive current flows through the top IGBT and the subsequent series-connected diode beneath it and vice versa for the negative current. During the voltage blocking (off-state), the top IGBT and the anti-parallel diode (or the Bottom IGBT and the antiparallel diode) are in forward and reverse blocking mode respectively dependent on the applied voltage to the SSCB (between point A and B).

Topology TP6 consists of two IGBTs [9] (anti-parallel diode is redundant for this topology but is shown here as most of the commercial IGBT modules normally have a diode connected in anti-parallel) and two diodes. This topology would also need the diodes connected in series with the IGBTs. The diodes will need to have the reverse voltage blocking capability to be at least the same as the forward voltage blocking rating of the IGBTs. However, the need for the series-connected diode can be eliminated if reverse blocking IGBTs (RB-IGBTs) are used. During the current conduction (on-state), the upper branch carries the positive current and the lower branch carries the negative current. During the voltage blocking (off-state), the IGBT in the upper branch is in forward blocking mode and the diode in the lower arm is in the reverse blocking mode and vice versa.

Topology TP7 is a novel topology, which aims to minimise on-state conduction losses during nominal current operation due to the use of Low Voltage (LV) rated Si MOSFETs. It consists of three different types of switches namely SAS, SMS, and STS. SMS and STS are known as Semiconductor Main Switch and Semiconductor Transfer Switch respectively. During the normal operation, the current flows through the SMS and STS branch. During over-current transient, STS breaks the over-current in the SMS/STS branch. The current is then diverted to the SAS branch for a short while before SAS also breaks the current. SAS is known as the Semiconductor Auxiliary Switch. The current is then eventually diverted to the MOV branch. However, the gate-control of various switches in this topology is quite complex as compared to other topologies. Further details about these topologies can be found in [5, 8].

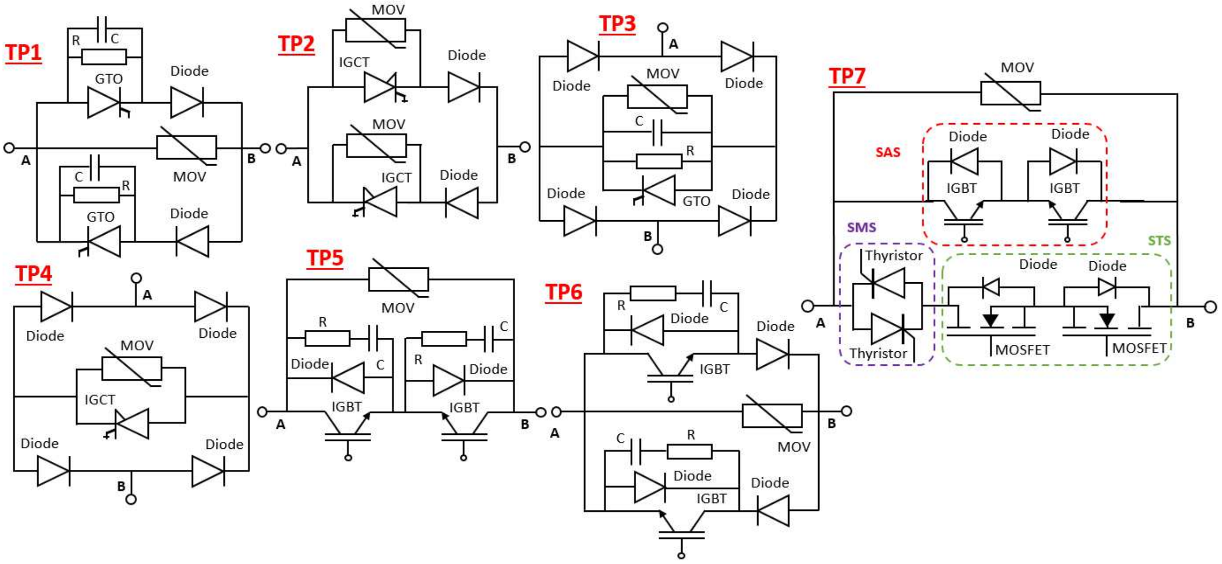

Figure 4: Schematic of the bi-directional DC SSCB Topologies (TP1 – TP7)

Thermal Analysis and Power Density Calculations for Different SSCB Topologies

In order to investigate the electro-thermal behaviour of semiconductor devices and their associated losses, different PLECs simulations have been carried out using different available semiconductor devices on the market. For performing the thermal simulations to obtain junction temperature estimates and conduction losses, highly accurate thermal models were needed to be generated in PLECs. Here, the different elements namely junction to case thermal impedance ($Z_{th(J-C)}$), case to heatsink thermal resistance ($R_{th(C-H)}$), and heatsink to ambient thermal resistance ($R_{th(H-A)}$) were all considered carefully as these values play a significant role within the steady-state and transient operation of a power module. The $R_{th(H-A)}$ was considered to be 0.01 ºC/W. During the steady-state operation of a power module, equation 1 below defines the maximum allowed power dissipation:

$$P_{D(max)} = \frac{T_{J(max)} - T_A}{R_{th}} \qquad \text{Equation 1}$$

Some of the thermal models were readily available on the manufacturers' website and the remaining were generated carefully using the information from the device's datasheet.

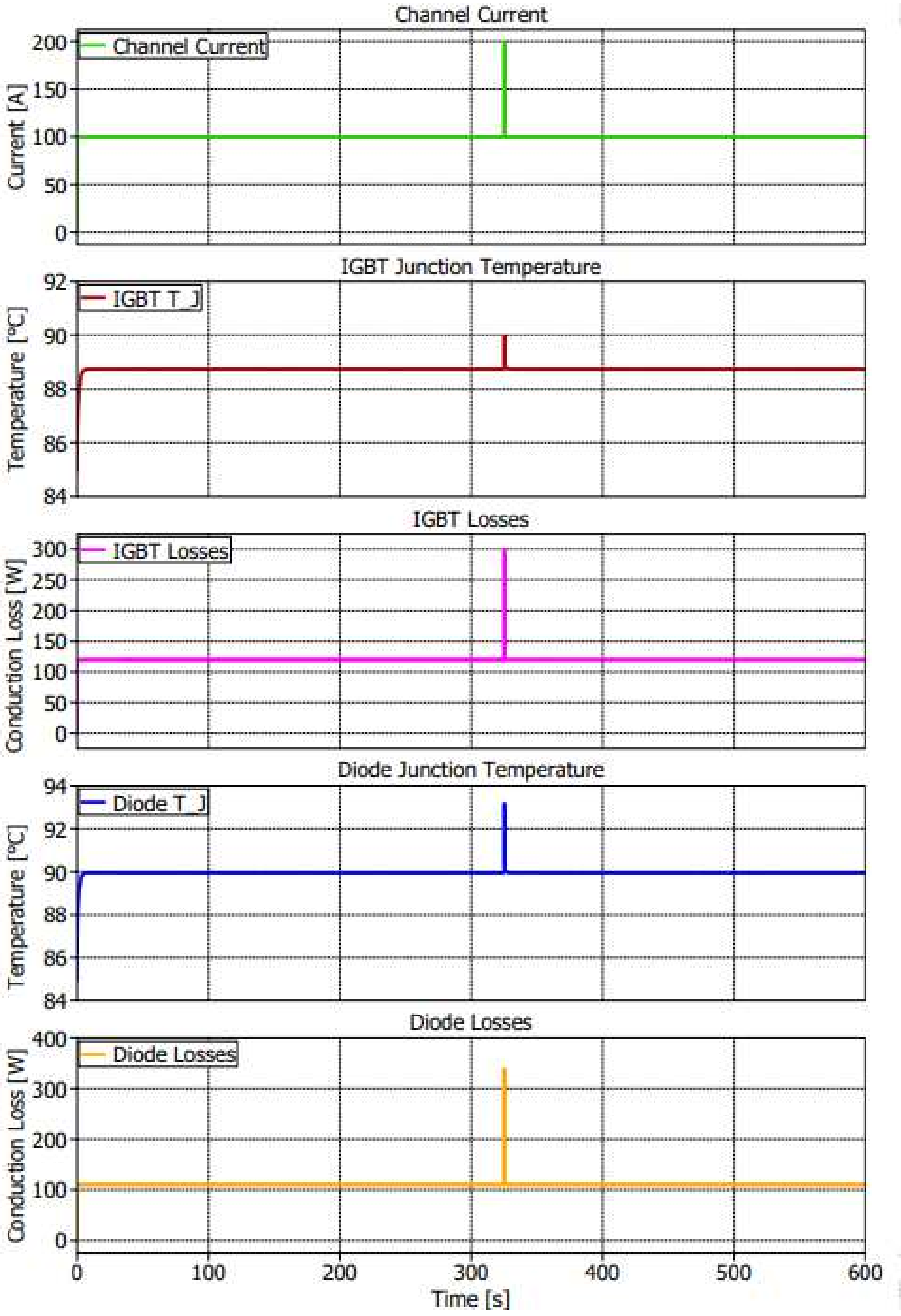

Figure 5: Simulation results using 4.5 kV rated Si IGBT

The test conditions used for these simulations are as follows: V_{DC} = 2400 V, nominal current I_{DC} = 100 A, Operating ambient Temperature T_A = 85 °C, L_{DC} = 100 µH, R_{DC} = 0.1 mΩ and $R_{th(H-A)}$ = 0.01 °C/W. For a better understanding of the overall simulation results presented here, simulation curves for one topology are included above. The simulation results for Topology TP5 using 4.5 kV, 800 A Si IGBT Module DIM800XSM45-TL000 from Dynex are included in Figure 5 above. Figure 5 shows the overall SSCB current (Channel current), IGBT Junction temperature ($T_{J(IGBT)}$), IGBT Conduction Losses ($P_{COND(IGBT)}$), Diode Junction Temperature ($T_{J(DIODE)}$), and Diode Conduction Losses ($P_{COND(DIODE)}$). The results presented here also show $T_{J(IGBT)}$ and $T_{J(DIODE)}$ for 2x the nominal current as well.

Simulations were carried out for Topologies TP1, TP2, TP5, and TP7. Topologies TP3 and TP4 with full diode rectifier configuration were not considered for simulation due to the additional power loss in the diode as mentioned earlier. Topology TP6 was also not simulated since it has a redundant anti-parallel diode connected with the IGBT, which is usually present in commercial IGBT modules but is not needed for this topology. Topology TP5 was simulated for three different types of devices including the SiC Power MOSFET from CREE. For TP5 with SiC MOSFETs, 1.7 kV half-bridge SiC Power Modules were used for simulation, therefore both switches inside the module would need to be utilized (to have voltage blocking of 3.4 kV) to obtain the required DC link voltage of 2.4 kV and also taking into account the voltage de-rating requirements. In addition, power to weight density was also analysed. The simulation results including the power losses and junction temperatures along with the power density values are summarised in Table II.

Topology TP2 has the lowest overall on-state losses of 122.1 W but due to the bulky weight of the IGCT module, power density figures are very low. Topology TP5 – 4.5 kV IGBT has slightly higher on-state losses of 230.0 W, however, its power density figure is much more promising than topology TP2. Topology TP1 has a good power density by weight of 80 W/g and its losses are comparable to TP5 – 4.5 kV IGBT topology. However, the gate drive circuit design is complex due to the gate drive current and speed requirements for turning off the GTO, which is quite difficult to meet [5]. Topology TP7 was simulated to see if it offers extremely low power losses due to the LV MOSFET. However, its losses are comparable to some of the other topologies such as TP5 – 4.5 kV IGBT. At the same time, it has relatively more complex gate drive control and possesses reliability concerns due to it involving various types of power devices.

Lastly, TP5 – 1.7 kV SiC MOSFETs have relatively higher losses but the power density by weight ratio is attractive. Here, two of the half-bridge 1.7 kV rated SiC MOSFET modules have to be connected in a common emitter configuration in order to achieve a maximum bi-directional voltage blocking capability of 3.4 kV. SSCB Architecture using MOSFET semiconductor devices can also benefit from the 3rd quadrant operation of the MOSFET using the device's channel instead of the current flowing through the anti-parallel body diode/Schottky diode which in turn helps to reduce conduction losses. The technique is normally termed active synchronous rectification. The high power losses seen for SiC simulations are due to the limitations on the commercial availability of SiC MOSFET modules above 1.7 kV voltage rating (3.3 kV and 4.5 kV SiC MOSFET modules – mainly exist as research samples) and low current ratings of the modules (which is essentially due to the existing low current ratings of the SiC bare dies). A bespoke 3.3 kV or higher rating SiC MOSFET power module will provide excellent power density by weight and volume values as well as lower overall conduction losses. But these two features of SiC devices at voltage levels above 1.7 kV are limited as device manufacturing technology is still improving to obtain the desired features at these voltage levels. Nonetheless, it is still achievable using a custom-made SiC module with a significant cost penalty. Moreover, overall losses for TP5 using 1.7 kV SiC MOSFETs could have been reduced further by connecting a further two MOSFET modules in parallel which would help reduce the overall resistance of the SSCB switches which would also reduce the conduction losses. However, paralleling MOSFETs come at a cost, such as: the semiconductor weight would double from 0.6 kg to 1.2 kg. Furthermore, connecting devices in series and parallel could have their own challenges since mismatch in electro-thermal device parameters between modules may affect voltage sharing during transient events [10, 11, 12].

Table II: Overall comparison of all simulated topologies in PLECS

#	Devices	Overall Conduction Losses (W)	Junction Temperature (°C) – (1x; 2x)	Total Semiconductor Weight (kg)	Power Density by Weight (W/g)
TP1	GTO (5SGF 30J4502) [13] and Diode (5SDD 08T5000) [14]	221.7	GTO: (88.8; 89.4) Diode: (90.1; 91.1)	3	80
TP2	IGCT (5SHY 50L5500) [15] and Diode (5SDD 08T5000) [14]	122.1	IGCT: (86.5; 86.7) Diode: (89.1; 90.1)	6.2	39
TP5	6.5 kV IGBT (DIM750ASM65-TS000) [16]	297.9	IGBT: (89.3; 90.4) Diode: (89.3; 90.6)	3.4	71
	4.5 kV IGBT (DIM800XSM45-TL000) [17]	230.0	IGBT: (88.7; 90.0) Diode: (90.0; 93.2)	2.2	109
	1.7 kV SiC MOSFETs – 2 modules (CAS300M17BM2) [18]	388.8	MOSFET-FC: (97.3; 112.1) MOSFET-Q3: (94.2; 99.8)	0.6	400
TP7	STS: MOSFET (IXFN360N10T) [19] SMS: Thyristor (TZ240N) [20] SAS: Si IGBT (IXYL60N450) [21] and Diode (GB50MOS17-247) [22]	244.4	Thyristor: (97.6; 100.3) MOSFET: (99.4; 117.0) Body Diode: (111.4; 125.7) IGBT: (---; 107.1) Diode: (---; 102.6)	1.968	-

Conclusion

This paper presents a detailed trade-off study for a 2.4 kV, 100 A rated DC SSCB for aerospace applications detailing different topologies and simulation results. A brief overview of the operation of a SSCB within a DC grid transmission network is presented followed by the possible bi-directional current conduction and voltage blocking DC SSCB topologies. The results of the thermal simulations in PLECs helped to obtain the on-state performance of the topologies. Additionally, the associated semiconductor weight for each simulated topology is also presented. From the obtained simulation results and the weight information, Topology TP5 – 4.5 kV Si IGBTs appears to be the most appropriate solution when considering all aspects of the analysis provided above. Moreover, Topology TP5 1.7 kV SiC MOSFETs is the next best candidate as its power density ratio is very attractive even though the conduction losses are higher. A better solution in terms of losses and weight using a bespoke SiC power MOSFET module having 3.3 kV or higher rating is potentially possible that would provide a more compact SSCB solution. However, the cost of a custom-made SiC MOSFET module ≥ 3.3 kV rating would be very expensive.

References

[1] Buticchi, Giampaolo, Serhiy Bozhko, Marco Liserre, Patrick Wheeler, and Kamal Al-Haddad. "On-board microgrids for the more electric aircraft—Technology review." *IEEE Transactions on Industrial Electronics* 66, no. 7 (2018): 5588-5599.
[2] Zhang, Chunlong, Hongyan Xing, Pengfei Li, Chunying Li, Dongbo Lv, and Shaojie Yang. "An Experimental Study of the Failure Mode of ZnO Varistors Under Multiple Lightning Strokes." Electronics 8, no. 2 (2019): 172.
[3] Mardira, Karl Primardi, Tapan K. Saha, and Roberta A. Sutton. "The effects of electrical degradation on the microstructure of metal oxide varistor." In 2001 IEEE/PES Transmission and Distribution Conference and Exposition. Developing New Perspectives (Cat. No. 01CH37294), vol. 1, pp. 329-334. IEEE, 2001.
[4] Molligoda, Devinda A., Pradip Chatterjee, Chandana J. Gajanayake, Amit Kumar Gupta, and K. J. Tseng. "Review of design and challenges of DC SSPC in more electric aircraft." In *2016 IEEE 2nd Annual Southern Power Electronics Conference (SPEC)*, pp. 1-5. IEEE, 2016.
[5] Meyer, Christoph, Stefan Schroder, and Rik W. De Doncker. "Solid-state circuit breakers and current limiters for medium-voltage systems having distributed power systems." *IEEE transactions on power electronics* 19, no. 5 (2004): 1333-1340.
[6] Podlesak, T. F., H. Singh, K. Fonda, J. Creedon, G. L. Schofield, and F. O. Johnson. "MEGAWATT HIGH SPEED SOLID STATE CIRCUIT BREAKER FOR PULSE POWER APPLICATIONS." In Ninth IEEE International Pulsed Power Conference, vol. 2, p. 984. IEEE, 1993.
[7] Schmerda, Richard F., Slobodan Krstic, Edward L. Wellner, and Ashish R. Bendre. "IGCTs vs. IGBTs for circuit breakers in advanced ship electrical systems." In *2009 IEEE Electric Ship Technologies Symposium*, pp. 400-405. IEEE, 2009.
[8] Gu, Chunyang, Pat Wheeler, Alberto Castellazzi, Alan J. Watson, and Francis Effah. "Semiconductor devices in solid-state/hybrid circuit breakers: current status and future trends." *Energies* 10, no. 4 (2017): 495.
[9] Vodyakho, O., M. Steurer, C. Edrington, G. Karady, B. Chowdhury, and S. Bhattacharya. "Design of a solid state fault isolation device for implementation in power electronics based distribution systems." In 41st North American Power Symposium, pp. 1-6. IEEE, 2009.
[10] Fayyaz, Asad, Besar Asllani, Alberto Castellazzi, Michele Riccio, and Andrea Irace. "Avalanche ruggedness of parallel SiC power MOSFETs." Microelectronics Reliability 88 (2018): 666-670.
[11] Castellazzi, Alberto, Asad Fayyaz, and Rainer Kraus. "SiC MOSFET device parameter spread and ruggedness of parallel multichip structures." In Materials Science Forum, vol. 924, pp. 811-817. Trans Tech Publications Ltd, 2018.
[12] Vechalapu, Kasunaidu, Subhashish Bhattacharya, and Eddy Aleoiza. "Performance evaluation of series connected 1700V SiC MOSFET devices." In *2015 IEEE 3rd Workshop on Wide Bandgap Power Devices and Applications (WiPDA)*, pp. 184-191. IEEE, 2015.
[13] ABB, "5SGF 30J4502 Datasheet."
[14] ABB, "5SDD 08T5000 Datasheet."

[15] ABB, "5SHY 50L5500 Datasheet."

[16] Dynex, "DIM750ASM65-TS000 Datasheet."

[17] Dynex, "DIM800XSM45-TL000 Datasheet."

[18] Wolfspeed, "CAS300M17BM2 Datasheet."

[19] IXYS "IXFN360N10T Datasheet."

[20] Infineon "TZ240N Datasheet."

[21] IXYS "IXYL60N450 Datasheet."

[22] GeneSiC "GB50MOS17-247 Datasheet."